Cleveland State University
EngagedScholarship@CSU

Chemical & Biomedical Engineering Faculty
Publications

Chemical & Biomedical Engineering Department

9-2002

Accurate Quantification of Steady and Pulsatile Flow With Segmented K-Space Magnetic Resonance Velocimetry

Haosen Zhang
Cleveland State University

Sandra S. Halliburton
Cleveland State University

James R. Moore
Siemens Medical Solutions

Orlando P. Simonetti
Siemens Medical Solutions

Paulo R. Schvartzman
Cleveland Clinic Foundation

See next page for additional authors

Follow this and additional works at: https://engagedscholarship.csuohio.edu/encbe_facpub

Part of the Biomedical Engineering and Bioengineering Commons, and the Transport
Phenomena Commons

How does access to this work benefit you? Let us know!

Publisher's Statement
The final publication is available at Springer via http://dx.doi.org/10.1007/S00348-002-0475-y

Original Citation
Zhang, H., Halliburton, S. S., Moore, J. R., Simonetti, O. P., Schvartzman, P. R., White, R. D., , & Chatzimavroudis, G. P. (2002).
Accurate quantification of steady and pulsatile flow with segmented k-space magnetic resonance velocimetry. Experiments in Fluids,
33(3), 458 - 463.

Repository Citation
Zhang, Haosen; Halliburton, Sandra S.; Moore, James R.; Simonetti, Orlando P.; Schvartzman, Paulo R.; White, Richard D.; and Chatzimavroudis,
George P., "Accurate Quantification of Steady and Pulsatile Flow With Segmented K-Space Magnetic Resonance Velocimetry" (2002). *Chemical &
Biomedical Engineering Faculty Publications*. 83.
https://engagedscholarship.csuohio.edu/encbe_facpub/83

Authors

Haosen Zhang, Sandra S. Halliburton, James R. Moore, Orlando P. Simonetti, Paulo R. Schvartzman, Richard D. White, and George P. Chatzimavroudis

Accurate quantification of steady and pulsatile flow with segmented k-space magnetic resonance velocimetry

H. Zhang, S.S. Halliburton, J.R. Moore, O.P. Simonetti,
P.R. Schvartzman, R.D. White, G.P. Chatzimavroudis

Abstract Conventional non-segmented magnetic resonance phase velocity mapping (MRPVM) is an accurate but relatively slow velocimetric technique. Therefore, the aim of this study was to evaluate the accuracy of the much faster segmented k-space MRPVM in quantifying flow. The axial velocity was measured in four straight tubes (inner diameter: 5.6–26.2 mm), using a segmented MRPVM sequence with seven lines of k-space per segment. The flow rate and flow volume were accurately quantified (errors<5%) under steady (r^2=0.99) and pulsatile flow (r^2=0.98), respectively. The measured velocity profiles and flow rates from the segmented sequence agreed with those from the non-segmented (p>0.05). Changing the slice thickness or the field of view did not affect the accuracy of the measurements. The results of this study suggest that fast, segmented MRPVM can be used for accurate flow quantification.

1
Introduction

Hydrogen-based magnetic resonance (MR) imaging is routinely used to provide anatomical, functional, and velocimetric information non-invasively. This imaging modality is based on the fact that inside a strong magnetic field the magnetic moments of hydrogen nuclei (spinning protons) align (parallel and anti-parallel) with the direction of the magnetic field. The strong magnetic field causes the spinning protons to "precess", similarly to the way that a spinning top wobbles around its axis as a result of its spin and the gravitational force. The frequency of this precession depends on the strength of the magnetic field. Using radio-frequency pulses with a frequency equal to this precession frequency, the protons can be energetically excited. As they return to equilibrium, they emit a signal that can be detected and used to reconstruct an image. By applying a combination of magnetic field gradients in all three directions in space (slice selection direction, phase encoding direction, and frequency encoding direction) during the procedure, the position of the excited protons can be spatially encoded (Fig. 1). This encoding is essential in image acquisition and reconstruction. The raw data (from the received signal) are in the frequency domain (k-space). Each time the protons are excited and then return to equilibrium, the received signal is used to fill one line of k-space. For an image of 256×256 pixels, 256 k-space lines are normally needed (although there are ways to reduce this number). After the k-space is filled with the proper amount of data, a two-dimensional Fourier transform reconstructs the image in the spatial domain.

An important feature of MR (which is the focus of this text) is its ability to measure flow velocity in any spatial direction via a technique called magnetic resonance phase velocity mapping (MRPVM). By applying proper bipolar magnetic field gradients (Fig. 1), the velocity of the protons can be encoded in the phase of the received signal (Moran 1982). This phase-velocity encoding follows a linear equation:

$$\phi = (\gamma M_1)v = \left(\gamma \int_0^{TE} G(t)t\,\mathrm{d}t \right) v = (\gamma A_g T)v \qquad (1)$$

where ϕ is the phase of the received signal (rad), γ is the gyromagnetic ratio (Hz/T), v is the velocity (assumed constant) (m/s), M_1 is the first moment of the gradient waveform (T s^2/m) at the echo time (TE), $G(t)$ is the magnetic field gradient (T/m), A_g is the "area" of each lobe of the bipolar gradient (T/m s), and T is the time between the centers of the two lobes of the gradient (s). The magnitude of the acquired signal is used to reconstruct the magnitude (anatomic) image, whereas the phase of the signal can be used to reconstruct a velocity map.

H. Zhang, S.S. Halliburton, G.P. Chatzimavroudis (✉)
Laboratory of Biofluid Mechanics and Cardiovascular Imaging,
Department of Chemical Engineering,
Cleveland State University,
1960 East 24th Street, Stilwell Hall 455,
Cleveland, OH 44115-2425, USA
E-mail: g.chatzimavroudis@csuohio.edu
Tel.: +1-216-6875396
Fax: +1-216-6879220

H. Zhang, S.S. Halliburton, P.R. Schvartzman, R.D. White,
G.P. Chatzimavroudis
Section of Cardiovascular Imaging,
Division of Radiology,
The Cleveland Clinic Foundation,
Cleveland, Oh., USA

J.R. Moore, O.P. Simonetti
Magnetic Resonance Division,
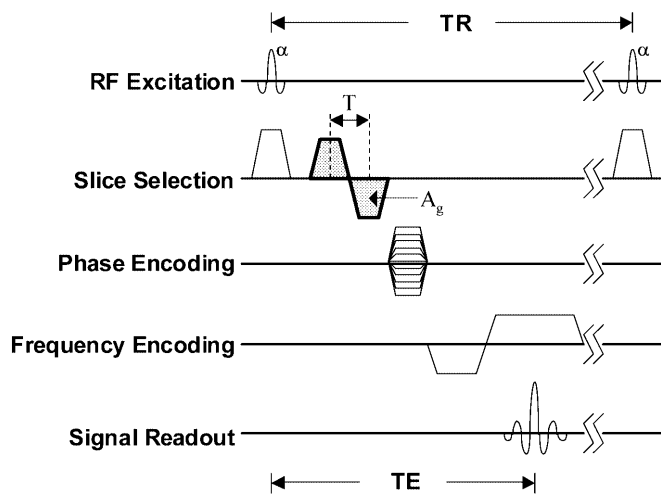Siemens Medical Solutions,
Chicago, Ill., USA

Fig. 1. Simplistic diagram of a typical non-segmented gradient-echo sequence with a bipolar gradient (shaded area) in the slice selection direction for velocity encoding (α: flip angle, *TR*: repetition time, *TE*: echo time, A_g: bipolar gradient single lobe area, *T*: time between the lobe centers in the bipolar gradient)

The velocimetric capability of MR has been widely used clinically (Pelc et al. 1992; Bogren and Buonocore 1994; Chatzimavroudis et al. 1998a; Kilner et al. 1993), but also in non-biomedical applications, such as to characterize the velocity profiles of pure fluids and suspensions (Corbett et al. 1995), to study flow in porous media (Mansfield et al. 1992), to visualize flow in fixed-bed reactors (Mantle et al. 2001), as a rheological technique (Britton and Callaghan 2000) and viscometer (Arola et al. 1997), and in other fluid mechanics applications. The accuracy of MRPVM has been sufficiently high, with errors of less than 10% under both steady and pulsatile flow conditions (Duerk and Pattanu 1988; Meier et al. 1988; Chatzimavroudis et al. 1997; Chatzimavroudis et al. 1998b; Moser et al. 2000). Clinical studies evaluating the potential and reliability of MRPVM for blood flow characterization or quantification have shown good correlations between MRPVM and conventional velocimetric (Doppler ultrasound) and flowmetric techniques (Meier et al. 1988; Dulce et al. 1992; Pelc et al. 1992).

Conventional MRPVM is performed using a gradient-echo sequence with a bipolar velocity-encoding gradient in the desired direction for velocity measurement (Fig. 1). In the case of pulsatile flow, such as arterial flow in the human body, multiple measurements are acquired during the (cardiac) cycle. The MR scanner can be triggered by the electrocardiogram (ECG) signal of the human subject to identify the beginning of the cardiac cycle, and then a number of image acquisitions are performed at different time points (time phases) throughout the cycle. For each time phase, only one excitation, spatial encoding, and signal readout is performed to fill one line in the k-space. To obtain the necessary number N of k-space lines for a successful image reconstruction under the desired spatial resolution, data must be acquired over N sequential heart beats. For example, for 128 k-space lines, the acquisition requires approximately 2 min, whereas for 256 lines, the acquisition requires approximately 4 min (depending on

heart rate and imaging parameters). Since blood flow measurement is usually only part of a complete cardiac MR examination and since new clinical protocols have started to involve multiple velocity acquisitions (Walker et al. 1995; Chatzimavroudis et al. 1998a; Walker et al. 2000), this single line non-segmented k-space technique becomes less practical clinically.

With the development of rapid imaging sequences, such as turbo gradient echo (TGE), the process of proton excitation, spatial encoding, and signal readout is performed very rapidly. Therefore, instead of acquiring only one k-space line for each time phase of the cardiac cycle and then wait until the next heart beat to acquire the next k-space line (non-segmented sequence), a segment of M k-space lines can be acquired very rapidly per time phase during each heart beat (segmented sequence). In other words, the segmented sequence is performed with such high speed that there is enough time to excite the protons, encode their position, and read the signal M times per time phase. As a result, for each time phase of the cardiac cycle, a segment of M k-space lines are obtained. Thus, to fill the total of N k-space lines, data must be acquired over N/M heart beats (instead of N heart beats for the non-segmented sequence). Consequently, if the number of lines per segment (M) is large enough, the acquisition can be performed in seconds instead of minutes, with high temporal and spatial resolution (Mohiaddin et al. 1995; Thomsen et al. 1995; Davis et al. 1997; Bock et al. 1998; Poutanen et al. 1998; Laffon et al. 1999). The larger the number (M) of lines per segment, the faster the acquisition. However, as the number of lines per segment increases, the temporal resolution of the acquired data becomes lower (less time phases can be acquired during the cardiac cycle as a result of the increase in the time interval assigned for each time phase).

If velocity-encoding gradients are added to the regular TGE sequence, the flow velocity can be measured rapidly. By placing an imaging slice perpendicular to the long axis of a tube and by measuring the axial velocity profile, the flow rate can be calculated by integrating the velocity over the cross-sectional area of the tube. If the flow is pulsatile, integration of the flow rate over the duration of a cycle results in the calculation of the flow volume per cycle.

The aim of this in vitro study was to evaluate the accuracy of segmented k-space TGE MRPVM in quantifying flow from through-plane velocity measurements, under a variety of flow conditions and imaging parameters.

2
Methods

2.1
Instrumentation, models, and flow set-up
Steady and pulsatile water flow experiments were conducted in a 1.5 T Siemens Sonata whole-body MRI scanner (Siemens Medical Systems, Erlangen, Germany) with a maximum gradient strength of 40 mT/m. MRPVM measurements were performed in four straight rigid PVC tubes with inside diameters of 5.6 mm (tube No. 1), 14.7 mm (tube No. 2), 20.2 mm (tube No. 3), and 26.2 mm (tube

No. 4). The tubes were placed in a water-filled container to assure detection of adequate signal.

Steady flow studies were first performed using a range of flow rates (1.7–16.7 ml/s for tube No. 1; 6.7–116.7 for tube No. 2; 10–166.7 ml/s for tube No. 3; and 16.7–200 ml/s for tube No. 4). The Reynolds number (*Re*) ranged between ~400 and ~10,500. The true flow rate was known via pre-calibrated rotameters. Then, pulsatile flow studies were conducted using a computer-controlled piston pump (SuperPump, SPS 3891, Vivitro Systems Inc., Victoria, BC, Canada) to provide flow pulsatility. A hardware/software system (Vivigen Waveform Generator VG8991, Vivitro Systems Inc.) was used to program and download the flow waveform from a PC to the piston pump. The piston stroke volumes studied were 6 ml/cycle for tube No. 1, 20 and 30 ml/cycle for tube No. 2, 40 and 60 ml/cycle for tube No. 3, and 70 and 90 ml/cycle for tube No. 4, all under a rate of 60 cycles/min. The true flow waveform was measured with a pre-calibrated, MR-compatible (brass), transit-time ultrasonic flow probe (20 N in-line, Transonic Systems, Inc., Ithaca, N.Y.). The flow data from the probe was acquired by a single channel flow meter (T-106, Transonic Systems Inc.). The flow waveform was recorded on a PC by digitizing the analog signal from the flow meter with an A/D board (PCI-MIO-16E-4, National Instruments Inc., Austin, Tex.), using the LabVIEW software (Version 5.0, National Instruments, Inc.). Integration of the flow curve during the cycle provided the true flow volume.

2.2
Imaging procedure
The test section (water-filled container with submerged straight tubes) was connected to the (steady or pulsatile) flow loop, and the entire system was inserted into the bore of the scanner with the test section placed at the iso-center (Fig. 2). A phased-array receiver coil was used to cover the test section to improve image quality. Initial localizer images showed the exact location of the tubes in the scanner bore. Then, an imaging slice was placed perpendicular to the long axis of the tube under study. MRPVM acquisitions of the through-plane velocity were performed for each flow condition, using the following two sequences: (a) conventional non-segmented gradient echo with one k-space line per time phase; and (b) segmented TGE with seven k-space lines per time phase. Both acquisitions were performed using a flip angle of 30°. The slice thickness (ST) was 5 and 3 mm, and the field of view (FOV) was 200×200 and 300×300 mm². The acquisition matrix was 192×256 for sequence (a) and 140×256 for sequence (b).
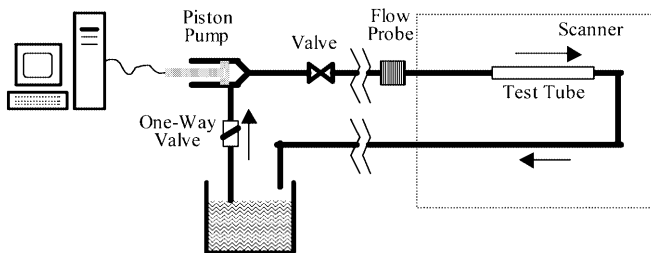

Fig. 2. The pulsatile flow loop

The actual voxel size varied from 1.0×0.8×3 to 1.6×1.2×5 mm³ for sequence (a) and from 1.4×0.8×3 to 2.1×1.2×5 mm³ for sequence (b). After interpolation, and for a reconstructed matrix of 256×256, the voxel size ranged from 0.8×0.8×3 to 1.2×1.2×5 mm³. The TE was varied between 2.3 and 3.5 ms (shortest possible based on other imaging parameters), whereas the temporal resolution was 30 ms for sequence (a), and 40–55 ms for sequence (b). The velocity-encoding value was 20–150 cm/s, depending on the magnitude of the flow.

In pulsatile flow, a TTL signal synchronized with the piston pump flow waveform triggered the scanner to acquire multiple measurements (time phases) throughout the cycle. The procedure was similar to the standard clinical situation in which the ECG signal from the subject is used to trigger the scanner for data acquisition. The time corresponding to each time phase was the time of acquisition of the central line of the segment. The number of time phases during the 1-s cycle was 34 for sequence (a), and 17–25 for sequence (b). The scanning duration was 3.2 min for sequence (a), and 20 s for sequence (b).

2.3
Image data analysis
All (magnitude and phase) images were transferred to a work station (Ultra-10, SUN Microsystems, Inc., Santa Clara, Calif.). First, a computer program converted the phase values of the phase images to velocity values, based on Eq. (1). Then the images were visualized using Transform (Version 3.4, Research Systems, Inc., Boulder, Colo.). The tube cross-section was clearly visualized and selected on the magnitude images, this selection was copied on the velocity images, and the fluid velocity was integrated over the tube cross-sectional area to find the flow rate. In pulsatile flow, integration of the flow curve over the cycle provided the flow volume.

Regression analysis, sign tests, and Bland–Altman analysis were performed to compare: (i) the MRPVM-measured flow values (from both sequences) with the true flow values; (ii) the MRPVM-measured flow values from the segmented technique with those from the non-segmented technique; and (iii) the flow results between different values for slice thickness and field of view. Minitab (Version 13, Minitab, Inc., State College, Penn.) was used for the statistical analysis. A *p*-value <0.05 would show significant difference.

3
Results
Figure 3 shows a magnitude and a phase (velocity) image acquired using MRPVM. The images were of sufficient quality for quantitative analysis. Figure 4 shows the measured centerline velocity profiles for the non-segmented and segmented acquisitions for laminar (*Re*=580) and non-laminar (*Re*=5250) flow. The velocity was normalized with respect to the cross-sectional average velocity. The velocity profiles from the segmented technique agree closely with the profiles from the non-segmented technique. As expected, the laminar flow profile is parabolic (Fig. 4a) with a maximum centerline velocity approximately twice the cross-sectional average velocity. The
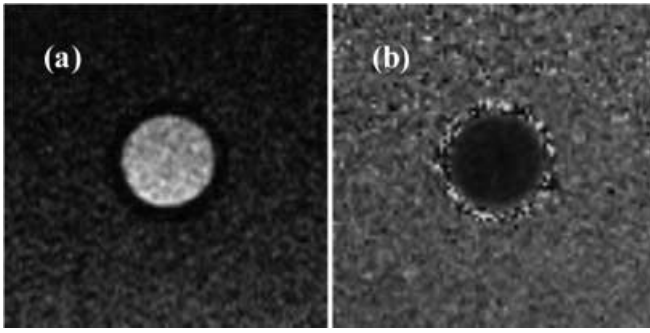
Fig. 3. Magnitude **a** and phase **b** MRPVM images clearly showing the cross-section of the tube. The phase image contains the velocity (encoded into the signal phase, according to Eq. 1)
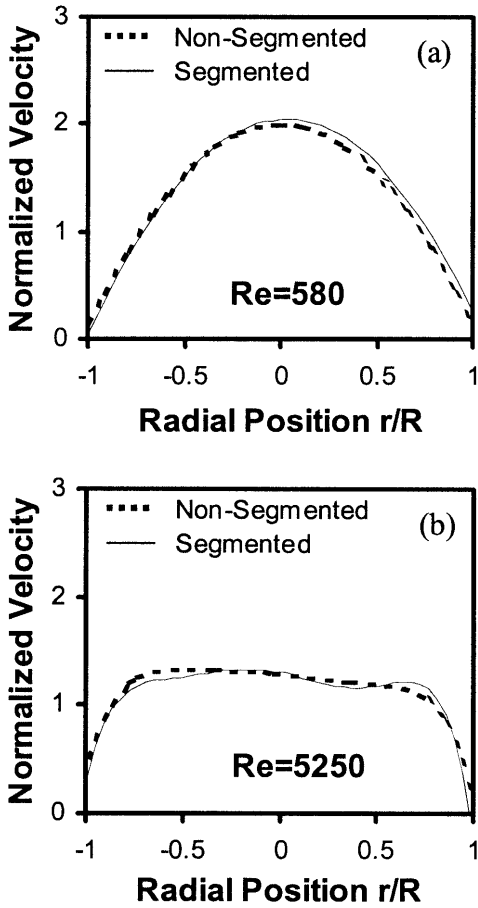

Fig. 4a, b. Normalized velocity profiles using the non-segmented (slow) sequence and the segmented (ultra-fast) sequence with 7 k-space lines per segment, for **a** laminar and **b** non-laminar flow. Normalization was performed by dividing the local velocity values with the average cross-sectional velocity

Fig. 5. **a** Comparison between the measured flow rates with the segmented MRPVM sequence and the true flow rates under steady flow conditions; **b** measured flow waveforms under pulsatile flow conditions for a true flow volume of 70 ml/cycle (measured flow volume =72 and 76 ml/cycle for the non-segmented and the segmented sequences, respectively); **c** comparison between the measured flow volumes with the segmented MRPVM sequence and the true flow volumes under pulsatile flow conditions

non-laminar flow profile is flatter (Fig 4b) with a maximum velocity approximately 1.4 times the cross-sectional average velocity.

3.1
Steady flow results
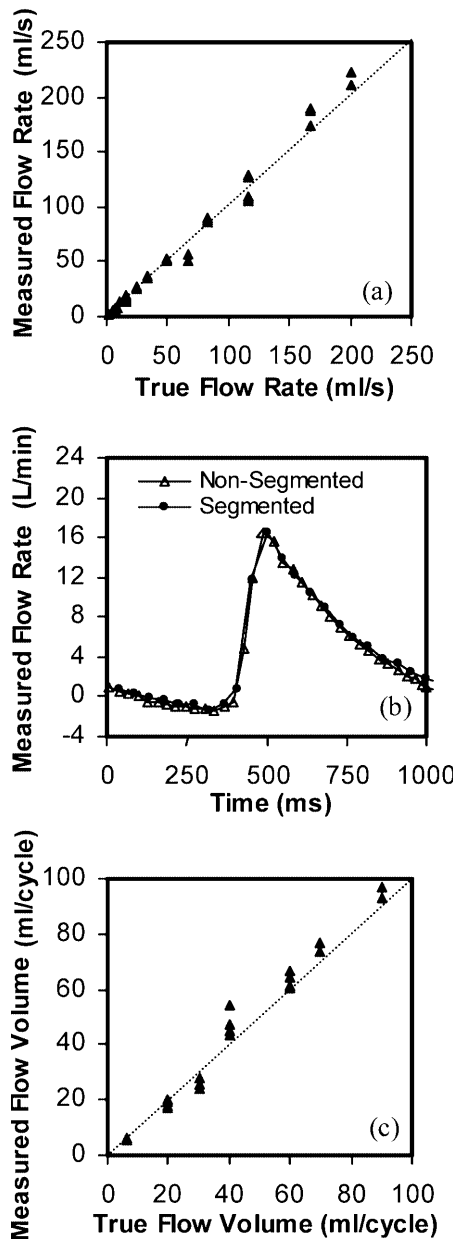Figure 5a shows the comparison between the flow rates measured with the segmented sequence and the true flow rates known from rotameters. The average error [(measured-true)/true] was –0.9%, and the regression line was $Y=1.05X–0.89$, $r^2=0.989$, $SE=6.5$ ml/s (Y: measured flow rate, X: true flow rate). The agreement between measured and true flow rates was confirmed by a sign test (p-value=0.21).

The measured flow rates from the non-segmented and the segmented sequence were also directly compared. Regression analysis ($Y=1.03X–0.74$, $r^2=0.997$, $SE=3.3$ ml/s; Y: segmented, X: non-segmented) and a sign test (p-value=0.89) showed a very close agreement.

3.2
Pulsatile flow results

Figure 5b shows the measured flow waveforms, using the non-segmented and segmented sequences, for a true flow volume of 70 ml/cycle. The measured flow volumes for the non-segmented and the segmented sequence were 72 and 76 ml/cycle, respectively. The flow curves for the two sequences were very similar both qualitatively and quantitatively for all flow conditions examined.

Figure 5c shows the comparison between the measured flow volumes with the segmented sequence and the true flow volumes known from the flow probe. The average error [(measured-true)/true] was 0.8%, and the regression line was $Y=1.09X-1.96$, $r^2=0.980$, $SE=4.1$ ml/cycle (Y: measured flow volume, X: true flow volume). This agreement was confirmed by a sign test (p-value=1.00). In addition, Fig. 6 shows the Bland–Altman analysis plot for the comparison between the measured flow volumes with the segmented sequence and the true flow volumes. The mean and the standard deviation are low (approximately 0.2 and 3.2 ml/cycle, respectively), and the data points are essentially all within the "±2 standard deviation" lines.

Direct comparison between the calculated flow volumes from the non-segmented and the segmented sequence showed no significant difference. The regression line was $Y=1.03X+1.00$, $r^2=0.948$, $SE=6.6$ ml/cycle (Y: segmented, X: non-segmented) and the sign test p-value 0.15.

3.3
Slice thickness and field of view

No difference was found between the measured flow rates with the segmented sequence for the two slice thickness values used (3 and 5 mm). The regression line on the steady flow data was $Y=1.06X-1.35$, $r^2=0.998$, $SE=2.9$ ml/s (Y: data for $ST=5$ mm, X: data for $ST=3$ mm). A similar finding was observed in the pulsatile flow case ($Y=1.01X+0.30$, $r^2=0.979$, $SE=4.4$ ml/cycle; Y: data for $ST=5$ mm, X: data for $ST=3$ mm). A sign test confirmed the agreement (p-value=0.61).

Similarly, no difference was found between the measurements for the two FOV values used (200 and 300 mm). The regression line was $Y=1.00X+0.20$, $r^2=1.000$, $SE=1.4$ ml/s (Y: data for FOV=300 mm, X: data for

FOV=200 mm), in steady flow, and $Y=1.01X+0.30$, $r^2=0.979$, $SE=4.4$ ml/cycle (Y: data for $ST=5$ mm, X: data for $ST=3$ mm), in pulsatile flow. The sign test p-value was 0.54.

4
Discussion

Magnetic resonance phase velocity mapping is being used to measure blood velocity profiles and flow non-invasively in the clinical field, as well as to characterize and quantify fluid mechanics in a number of non-medical applications. Despite its established accuracy (shown through a number of experimental and clinical studies), conventional non-segmented MRPVM is relatively slow. It takes minutes for a single-slice, one-directional velocity measurement. This is too long within new clinical protocols that have started to involve multiple velocity acquisitions. Therefore, ultra-fast MRPVM is necessary. This study evaluated the accuracy of a segmented MRPVM acquisition scheme with seven k-space lines per segment, by comparing the flow results with those acquired using the conventional non-segmented sequence and with true flow values. MRPVM measurements under steady and pulsatile flow conditions showed that the seven-line segmented sequence provided very accurate and reliable results.

Seven k-space lines per segment allowed a complete cine acquisition of 17–25 cardiac "phases" in 20 s for a rate of 60 cycles/min. Increasing the number of lines per segment beyond seven would further shorten the scan time, at the expense, however, of temporal resolution (fewer time phases per cycle acquired). In addition, by increasing the number of lines, the acquisition time window per time phase becomes wider; this can cause problems in adequately resolving rapidly changing flow waveforms, such as that in the aorta during systole. On the other hand, by decreasing the number of lines per segment, the temporal resolution improves, at the expense of scanning time. As an example, and for the sequence used in this study, selecting five (instead of seven) lines per segment would lead to a ≈30-s breath-hold acquisition, probably too long for certain patients. Therefore, implementation of ultra-fast techniques should be done after a complete evaluation of the accuracy of the sequence, placing particular emphasis on proper scan duration and temporal resolution.

The good image quality observed for both sequences and for all flow conditions was essential for a reliable image analysis and processing. The measured velocity profiles agreed qualitatively and quantitatively with what is theoretically and empirically expected (parabolic profiles for laminar flow with a centerline velocity approximately twice as large as the average cross-sectional velocity; flat-like profiles for non-laminar flow with the maximum velocity significantly less than twice the cross-sectional average velocity), reflecting the reliability of segmented MRPVM in measuring velocity. There was a small asymmetry in the velocity profiles at the wall (the velocity at $r/R=-1$ was different from that at $r/R=1$), probably due to partial volume effects (Fig. 4). The pixels corresponding to locations $r/R=-1$ and $r/R=1$ may be exclusively in the lumen, or partially in the lumen and partially in the wall. If
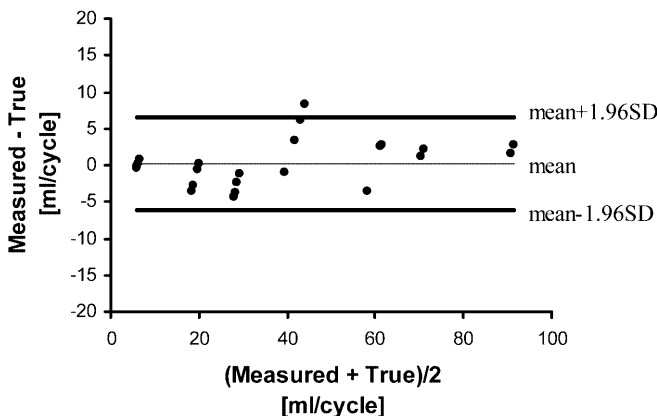

Fig. 6. Bland–Altman analysis plot comparing the measured and true flow volumes for the seven-line segmented sequence

the portion of the pixel being in the wall is different in those two locations, the measured velocity values will be different. Therefore, it is not surprising to observe slight asymmetries in the profile. Increasing the spatial resolution (linked to further advancement in hardware/software) and, at the same time, maintaining image quality will reduce this problem and will allow reliable velocity acquisitions very close to the wall (very important for accurate calculations of the wall shear stress).

In pulsatile flow, the measured flow curves for both the segmented and the non-segmented sequence were very similar (Fig. 5b). For the segmented sequence, since the most useful information is contained in the most central line of the segment, there was an adjustment so that the time corresponding to any time phase would be the time of acquisition of the central k-space line of the segment. This adjustment was necessary to avoid a temporal shift of the flow curves, as previously observed (Poutanen et al. 1998).

5
Conclusions

Steady and pulsatile flow experiments in straight rigid tubes under a variety of conditions showed that segmented k-space MRPVM can provide very accurate, ultra-fast velocity measurements and flow quantification. The calculated flow rates and flow volumes agreed very closely with the true flow values. Results for the velocity profiles under laminar and non-laminar flow showed the qualitative and quantitative reliability of the technique in measuring the flow velocity. As the need for faster non-invasive flow velocity measurements is increasing, segmented k-space MRPVM shows great potential for fast and accurate flow quantification.

References

Arola DF, Barrall GA, Powell RL, McCarthy KL, McCarthy MJ (1997) Use of nuclear magnetic resonance imaging as a viscometer for process monitoring. Chem Eng Sci 52:2049–2057

Bock M, Schoenberg SO, Schad LR, Knopp MV, Essig M, van Kaick G (1998) Interleaved gradient-echo planar (IGEPI) and phase contrast CINE-PC flow measurements in the renal artery. J Magn Reson Imaging 8:889–895

Bogren HG, Buonocore MH (1994) Blood flow measurements in the aorta and major arteries with MR velocity mapping. J Magn Reson Imaging 4:119–130

Britton MM, Callaghan PT (2000) NMR velocimetry study of the temperature dependent rheology of butter, semisoft butter and margarine. J Texture Stud 31:245–255

Chatzimavroudis GP, Oshinski JN, Franch RH, Pettigrew RI, Walker PG, Yoganathan AP (1998a) Quantification of the aortic regurgitant volume with magnetic resonance phase velocity mapping: a clinical investigation of the importance of imaging slice location. J Heart Valve Dis 7:94–101

Chatzimavroudis GP, Oshinski JN, Pettigrew RI, Walker PG, Franch RH, Yoganathan AP (1998b) Quantification of mitral regurgitation with MR phase-velocity mapping using a control volume method. J Magn Reson Imaging 8:577–582

Chatzimavroudis GP, Walker PG, Oshinski JN, Franch RH, Pettigrew RI, Yoganathan AP (1997) Slice location dependence of aortic regurgitation measurements with MR phase velocity mapping. Magn Reson Med 37:545–551

Corbett AM, Phillips RJ, Kauten RJ, McCarthy KL (1995) Magnetic resonance imaging of concentration and velocity profiles of pure fluids and solid suspensions in rotating geometries. J Rheol 39:907–924

Davis CP, Liu P-F, Hauser M, Göhde SC, von Schulthess GK, Debatin JF (1997) Coronary flow and coronary flow reserve measurements in humans with breath-held magnetic resonance phase contrast velocity mapping. Magn Reson Med 37:537–544

Dulce M-C, Mostbeck GH, O'Sullivan M, Cheitlin M, Caputo GR, Higgins CB (1992) Severity of aortic regurgitation: interstudy reproducibility of measurements with velocity-encoded cine MR imaging. Radiology 185:235–240

Duerk JL, Pattanu PM (1988) In-plane flow velocity quantification along the phase encoding axis in MRI. Magn Reson Imaging 6:321–333

Kilner PJ, Yang GZ, Mohiaddin RH, Firmin DN, Longmore DB (1993) Helical and retrograde secondary flow patterns in the aortic arch studied by three-directional magnetic resonance velocity mapping. Circulation 88:2235–2247

Laffon E, Lecesne R, de Ledinghen V, Valli N, Couzigou P, Laurent F, Drouillard J, Ducassou D, Barat J-L (1999) Segmented 5 versus nonsegmented flow quantitation: comparison of portal vein flow measurements. Invest Radiol 34:176–180

Mansfield P, Bowtell R, Blackband S, Guilfoyle DN (1992) Magnetic resonance imaging: applications of novel methods in studies of porous media. Magn Reson Imaging 10:741–746

Mantle MD, Sederman AJ, Gladden LF (2001) Single- and two-phase flow in fixed-bed reactors: MRI flow visualisation and lattice-Boltzmann simulations. Chem Eng Sci 56:523–529

Meier D, Maier S, Bosiger P (1988) Quantitative flow measurements on phantoms and on blood vessels with MR. Magn Reson Med 8:25–34

Mohiaddin RH, Gatehouse PD, Firmin DN (1995) Exercise-related changes in aortic flow measured with spiral echo-planar MR velocity mapping. J Magn Reson Imaging 5:159–163

Moran PR (1982) A flow velocity zeugmatographic interlace for NMR imaging in humans. Magn Reson Imaging 1:197–203

Moser KW, Kutter EC, Georgiadis JG, Buckius RO, Morris HD, Torczynski JR (2000) Velocity measurements of flow through a step stenosis using magnetic resonance imaging. Exp Fluids 29:438–447

Pelc LR, Pelc NJ, Rayhill SC, Castro LJ, Glover GH, Herfkens RJ, Miller DC, Jeffrey RB (1992) Arterial and venous blood flow: noninvasive quantitation with MR imaging. Radiology 185:809–812

Poutanen V-P, Kivisaari R, Häkkinen A-M, Savolainen S, Hekali P, Standertskjöld-Nordenstam C-G (1998) Multiphase segmented k-space velocity mapping in pulsatile flow waveforms. Magn Reson Imaging 16:261–270

Thomsen C; Cortsen M; Söndergaard L; Henriksen O; Ståhlberg F (1995) A segmented k-space velocity mapping protocol for quantification of renal artery blood flow during breath-holding. J Magn Reson Imaging 5:393–401

Walker PG, Houlind K, Djurhuus C, Kim WY, Pedersen EM (2000) Motion correction for the quantification of mitral regurgitation using the control volume method. Magn Reson Med 43:726–733

Walker PG, Oyre S, Pedersen EM, Houlind K, Guenet FSA, Yoganathan AP (1995) A new control volume method for calculating valvular regurgitation. Circulation 92:579–586